Physics – Uspekhi **37** (10) 991 – 1004 (1994)

PACS numbers: 13.85.−t; 29.27.Hj; 12.38−b

Spin effects in hard processes with polarised protons

S M Troshin, N E Tyurin

Contents

Abstract. The dynamics of spin effects in hard hadron processes is discussed. Possibilities for the experimental study of the effects by means of accelerated, polarised proton beams are considered.

1. Introduction

The physics of hadron interactions involves the study of hadronic wave functions and the dynamics of the interaction of hadron constituents. The continuing current interest in spin effects and the spin structure of hadrons derives from their well-appreciated importance for the analysis and theoretical description of hadron interaction dynamics.

The concept of spin entered physics in the mid-twenties, when Uhlenbeck and Goudsmit introduced the electron's internal degree of freedom — spin — as a real physical property which had to replace the nonmechanical stress idea used by Pauli in formulating his Principle. The Uhlenbeck–Goudsmit formulation also allowed a classical mechanical interpretation of Pauli's new quantum number, and gave some insight into the anomalous Zeeman effect.

Thus, Pauli formulated the concept of a new quantum number, to fit in with his double-state idea, and Uhlenbeck and Goudsmit introduced the electron intrinsic momentum (i.e. spin) as a concept with physical reality.

S M Troshin, N E Tyurin Institute for High Energy Physics
142284 Protvino, Moscow Region
Tel. (7 096) 771 34 42; Fax (7 095) 230 23 37
E-mail: tyurin@mx.ihep.su

Received 20 July 1994, revised 5 September 1994
Uspekhi Fizicheskikh Nauk **164** (10) 1073 – 1087 (1994)
Translated by E Strel'chenko; revised by J R Briggs

The discovery of the Dirac equation showed spin to be an inherent property of relativistic theory. A free Dirac particle, with a wave function satisfying a matrix equation, has — in addition to the momentum — one further invariant, an intrinsic angular momentum (i.e. spin) equal to $\hbar/2$.

The concept of spin emerged at the intersection of ideas in classical and quantum physics. Its prototype is classical rotation. It is noteworthy that as far back as 1921 Compton made his calculations by treating the electron as an extended and rapidly spinning object. In actual fact, however, spin is an entirely quantum-mechanical concept.

The Pauli principle and the spin concept served as the starting point for fundamental ideas such as the interchange symmetry of wave functions, and statistics.

Until recently it was thought that one might be able to do without spin in high-energy physics. Even though the fundamental building blocks of matter (quarks, leptons, and particles by which fundamental interactions are mediated) are all of nonzero spin,

$$s=1/2: \quad \begin{pmatrix} \mathrm{u} \\ \mathrm{d} \end{pmatrix}, \ \begin{pmatrix} \mathrm{c} \\ \mathrm{s} \end{pmatrix}, \ \begin{pmatrix} \mathrm{t} \\ \mathrm{b} \end{pmatrix}, \ \begin{pmatrix} \nu_{\mathrm{e}} \\ \mathrm{e} \end{pmatrix}, \ \begin{pmatrix} \nu_{\mu} \\ \mu \end{pmatrix}, \ \begin{pmatrix} \nu_{\tau} \\ \tau \end{pmatrix},$$

$$s=1: \quad \gamma, \ \mathrm{W}^{\pm}, \ \mathrm{Z}^{0}, \ \mathrm{g},$$

the corresponding effects have generally been accounted for either via combinatorial analysis, in constructing state vectors, or by means of appropriate amplitude factors. The dynamical implications of spin degrees of freedom have invariably been ignored.

It is to be noted that high-energy experiments on spin effects have been widely considered as just keeping up the traditions of low-energy physics. On the other hand, one would expect that spin plays a significant role in quark–lepton interactions. Experimental spin physics has led to results which have strong implications for the theoretical concepts and models currently in use in the high-energy region.

The flow of new results in the eighties, particularly in the large-transverse-momentum ($p_\perp$) region, highlighted the problem of spin degrees of freedom in interaction dynamics while at the same time providing challenges to quantum chromodynamics, or more precisely its perturbative formulation, which is supposed to describe high-$p_\perp$ processes.

In perturbative quantum chromodynamics, the polarisation of a quark in a hard subprocess turns out to be small in view of the vector nature of the quantum chromodynamic interaction, and quark helicity conserves terms up to $O(m/\sqrt{s})$. Also, in explaining the observed asymmetries

$$A \sim \mathrm{Im}\,(F_{nf}F_f^*)\ ,$$

one finds that the required phase shifts for amplitudes with (F_f) or without (F_{nf}) a change in helicity, fail to be generated by short-distance interactions and are presumably of nonperturbative origin.

Much attention has been paid in recent years to nucleon spin structure, in particular to the role quarks and gluons play in the spin balance of the proton:

$$s_{\mathrm{p}} = s_{\mathrm{q}} + s_{\mathrm{g}} + \langle L \rangle\ .$$

The contributions made by the gluon spin and by the orbital momenta of quarks and gluons appear to be significant [1]. In addition to the SLAC and CERN results, new experiments are being planned to measure the spin structure functions of the proton and neutron to enable more decisive conclusions to be reached. The theoretical interpretation of the available results has already shed new light on the nature of nucleon spin [2].

The study of spin effects is one of the most topical problems in high-energy physics. The measurement of spin observables is more informative compared with spin-averaged quantities and allows a detailed analysis of existing theoretical models. A number of interesting results in this area are still waiting for an explanation. These include large values of spin–spin correlation and analysing power in elastic reactions [3], high hyperon polarisation [4], and large asymmetries in binary [5] and inclusive [6] processes. Furthermore, the appreciable sub-ISR hyperon polarisation indicates that spin effects remain quite large up to energies equivalent to 2 TeV in the laboratory frame. Figs 1–3 illustrate the important role of spin effects in hadron elastic scattering and production processes.

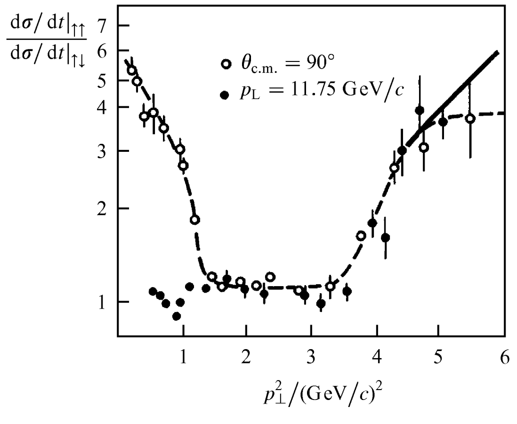

Figure 1. Cross section ratio for pure spin states in elastic pp scattering as a function of $p_\perp^2$, for fixed angle ($\theta_{\mathrm{c.m.}} = 90°$) and varying energy, and for fixed energy (11.75 GeV) and varying angle.

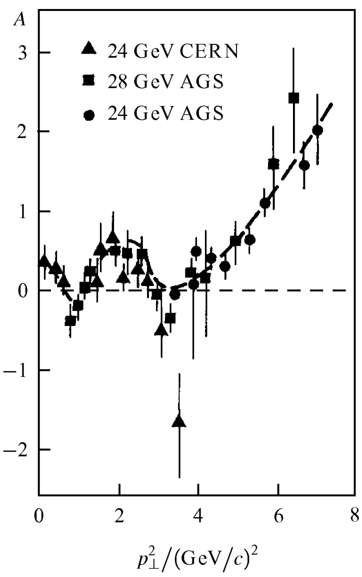

Figure 2. Analysing power A versus $p_\perp^2$ in elastic pp scattering at 24 and 28 GeV [3].

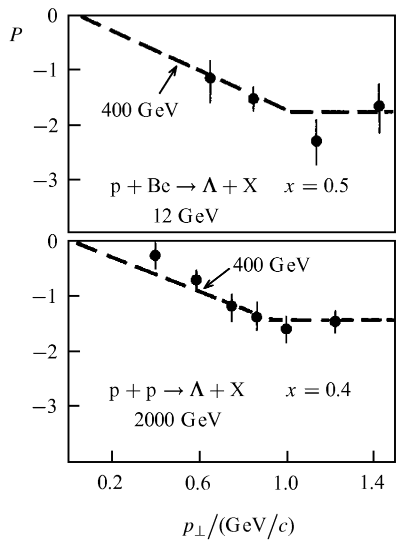

Figure 3. Λ-hyperon polarisation at 12 and 2000 GeV (equivalent fixed-target energy) versus $p_\perp$ [4].

Polarisation experiments began to be conducted in the early 50s. At present, spin experiments fall into three groups:

(1) unpolarised target, unpolarised beam;

(2) polarised target, unpolarised beam;

(3) polarised target, polarised beam.

The experiments in the first group are good for measuring the polarisation of unstable final particles such as Λ hyperons, which is determined from the parity-nonconserving decay $\Lambda \to \mathrm{p}\pi^-$. In the second group, polarised targets are needed, and the third group also requires that either accelerated polarised beams or polarised secondary beams be employed. In the polarisation experiments in the first and second groups one can measure polarisation and one-spin asymmetries, and in experiments in the third group spin – spin correlation parameters are also covered.

The simplest possible observable is the interaction-induced particle polarisation P. The polarisation is twice the averaged spin of the particle. For example, for a spin of 1/2 the polarisation is given by

$$P = \langle \boldsymbol{\sigma} \cdot \hat{\boldsymbol{p}}_i \times \hat{\boldsymbol{p}}_f \rangle \,, \tag{1}$$

where the vector $\hat{\boldsymbol{p}}_i \times \hat{\boldsymbol{p}}_f$ determines the normal $\hat{\boldsymbol{n}}$ to the scattering plane. To produce polarisation one uses polarised-target (or polarised-beam) experiments which yield a quantity A called analysing power. This is defined as the ratio

$$A = \frac{\mathrm{d}\sigma_{\uparrow} - \mathrm{d}\sigma_{\downarrow}}{\mathrm{d}\sigma_{\uparrow} + \mathrm{d}\sigma_{\downarrow}} \,. \tag{2}$$

Here $\mathrm{d}\sigma_{\uparrow}$ and $\mathrm{d}\sigma_{\downarrow}$ are the scattering cross sections on the polarised target, and $\uparrow$ and $\downarrow$ indicate the direction of the target polarisation relative to the scattering plane normal. A similar definition holds in the case of a polarised beam.

The time-reversal invariance has the consequence that in binary reactions the polarisation of the scattered particle, P, is equal to the analysing power $A: P = A$.

It should be noted that in some experiments, instead of changing the target (beam) polarisation direction, the scattering-induced left – right asymmetry is measured. This is defined by

$$A^{\mathrm{LR}} = \frac{\mathrm{d}\sigma_{\uparrow}(\theta) - \mathrm{d}\sigma_{\uparrow}(-\theta)}{\mathrm{d}\sigma_{\uparrow}(\theta) + \mathrm{d}\sigma_{\uparrow}(-\theta)} \,. \tag{3}$$

Left – right asymmetry equals analysing power for all processes which have only one single-helicity-flip amplitude, as for example in pp scattering.

One-spin asymmetries characterise the possibility of one of the particles changing its helicity in the interaction process and also characterise the relative phase of the helicity-flip and helicity-nonflip amplitudes.

In polarised-beam polarised-target experiments, spin – spin correlation parameters can be measured. These are proportional to the quantities $\langle \boldsymbol{\sigma}_1 \cdot \boldsymbol{\sigma}_2 \rangle$ and characterise the dependence of cross sections on particle spin directions. Spin – spin correlation parameters, say A_{ll}, are defined as follows:

$$A_{ll} = \frac{\mathrm{d}\sigma(\rightrightarrows)/\mathrm{d}t + \mathrm{d}\sigma(\leftleftarrows)/\mathrm{d}t - \mathrm{d}\sigma(\rightleftarrows)/\mathrm{d}t - \mathrm{d}\sigma(\leftrightarrows)/\mathrm{d}t}{\mathrm{d}\sigma(\rightrightarrows)/\mathrm{d}t + \mathrm{d}\sigma(\leftleftarrows)/\mathrm{d}t + \mathrm{d}\sigma(\rightleftarrows)/\mathrm{d}t + \mathrm{d}\sigma(\leftrightarrows)/\mathrm{d}t} \,, \tag{4}$$

where $\mathrm{d}\sigma(\rightrightarrows)/\,\mathrm{d}t$ is the differential cross section for the scattering of a polarised beam from a polarised target when the initial particles have their spins directed along the beam (z direction), i.e., $s_z^a = s_z^b = 1/2$. Another spin – spin correlation parameter, A_{nn}, is given by a formula similar to Eqn (4) and corresponds to the case of initial spins being oriented along the scattering plane normal ($\hat{n} = \hat{y}$). The parameter A_{ss} describes the configuration with spins along the third direction, $\hat{x}$. In each case, a summation over the spins of the final particles is carried out.

Further spin – spin correlation parameters may be constructed, to relate, for example, differently directed spins of the initial particles (A_{sl}), or the spin of an initial particle and that of a final one (parameters D_{nn} and K_{nn}).

In polarised-beam experiments, in addition to parameters that derive from differential cross sections, one can also measure integral characteristics, such as the difference in total cross section for interacting particles initially in different spin states. These quantities, $\Delta\sigma_{\mathrm{L}}$ and $\Delta\sigma_{\mathrm{T}}$, relate to the longitudinal and transverse orientations of initial-particle spins. They are defined as follows:

$$\Delta\sigma_{\mathrm{L}} = \sigma_{\mathrm{tot}}(\rightleftarrows) - \sigma_{\mathrm{tot}}(\rightrightarrows) = \sigma_{\mathrm{tot}}(++) - \sigma_{\mathrm{tot}}(+-) \,,$$
$$\Delta\sigma_{\mathrm{T}} = \sigma_{\mathrm{tot}}(\uparrow\uparrow) - \sigma_{\mathrm{tot}}(\uparrow\downarrow) \,. \tag{5}$$

In Eqn (5) the arrows indicate the spin direction of the initial hadrons, and the plus and minus signs denote the helicities of the $+1/2$ and $-1/2$ hadrons, respectively.

This review discusses the role of the spin degrees of freedom and the potential of spin effects for the study of the hadron structure and hadron interaction dynamics. The dynamical implications of spin effects in hadron reactions emphasise, in particular, the role of chiral symmetry breaking. The experimental results shown in Figs 1 to 3 are analysed, including the high analysing power A and the large value of the spin – spin correlation parameter A_{nn}. The possibility of studying spin effects with the aid of accelerated polarised proton beams is also discussed. See Ref. [7] for a more detailed discussion of the general approach to the problem of the spin degrees of freedom in the high-energy region.

2. Helicity conservation in quantum chromodynamics

As already noted, the objective of the theory of strong interactions is to study the hadron structure and hadron interaction dynamics. At present, quantum chromodynamics (QCD) is being considered as a suitable theory for the purpose.

The perturbation expansion used in calculating observable quantities [8] relies on the asymptotic freedom property of QCD. Generally, such calculations employ the parton model [9], which considers a hadron as a cluster of noninteracting, massless point constituents.

Perturbative chromodynamics makes it possible to describe spin-averaged observables for hadron interactions at short distances. Serious difficulties arise, however, when the observables under study involve spin degrees of freedom [10]. This is due to the chiral invariance of the QCD Lagrangian and the vector nature of the QCD interaction. In fact, the current quark masses are small and so the QCD Lagrangian

$$L_{\mathrm{QCD}} = -\tfrac{1}{4}\,\mathrm{Tr}\,(F_{\mu\nu}F^{\mu\nu}) + \bar{\psi}^f(x)\,(\mathrm{i}\gamma^{\mu}D_{\mu} - m_f)\,\psi^f(x) \tag{6}$$

is approximately invariant under the $\mathrm{SU}(3)_{\mathrm{L}} \times \mathrm{SU}(3)_{\mathrm{R}}$-group chiral transformations. For massless quarks, chirality and helicity are equal:

$$\psi_{\mathrm{R}} = \tfrac{1}{2}(1+\gamma_5)\psi \,, \quad \psi_{\mathrm{L}} = \tfrac{1}{2}(1-\gamma_5)\psi \,,$$
$$\psi_{1/2} = \psi_{\mathrm{R}} \,, \quad \psi_{-1/2} = \psi_{\mathrm{L}} \,. \tag{7}$$

QCD interactions are equal for left and right quarks,

$$\bar{\psi}\gamma_{\mu}\psi A^{\mu} = \bar{\psi}_{\mathrm{L}}\gamma_{\mu}\psi_{\mathrm{L}}A^{\mu} + \bar{\psi}_{\mathrm{R}}\gamma_{\mu}\psi_{\mathrm{R}}A^{\mu} \,, \tag{8}$$

and hence do not flip helicity.

Under such conditions massless particles will remain either left or right at all times. Including current quark masses yields a small helicity-flip amplitude and a very low quark polarisation,

$$P_{\mathrm{q}} \propto \frac{\alpha_s m}{Q} \,, \tag{9}$$

the latter originating from diagrams with nonzero imaginary parts.

The most commonly used tool for the QCD treatment of hard hadron processes is the factorisation theorem, which separates the dynamics of bound states at large distances from the interaction dynamics of the constituents at small distances. Clearly, the description of the hadronic wave function is an essentially nonperturbative problem.

In the general case a hadronic wave function can be represented as a Fock-state expansion [11]:

$$|h\rangle = \sum_{n,\lambda_i} \psi_n^h(x_i, \boldsymbol{k}_{\perp i}, \lambda_i)\,|n\rangle\,, \tag{10}$$

where $|n\rangle$ is the n-parton Fock state and the functions $\psi_n^h(x_i, \boldsymbol{k}_{\perp i}, \lambda_i)$ are a set of parton amplitudes defined on the free-quark free-gluon Fock basis for equal light-cone 'times' $\tau = t + z$. In this expansion $\boldsymbol{k}_{\perp i}$ is the transverse momentum of the ith quark or gluon relative to the bound state momentum $\boldsymbol{P}$, and x_i is the corresponding light-cone momentum fraction,

$$x_i = \frac{k_i^+}{P^+} \equiv \frac{(k^0 + k^3)_i}{P^0 + P^3}\,,$$

which in the infinite-momentum frame is the fraction of the parton's longitudinal momentum. The parton-amplitude normalisation condition is of the form

$$\sum_{n,\lambda_i} \int [\mathrm{d}x]\,[\mathrm{d}^2k_\perp]\,|\psi_n^h(x_i, \boldsymbol{k}_{\perp i}, \lambda_i)|^2 = 1\,,$$

where $[\mathrm{d}^2k_\perp]$ denotes integration over the transverse momenta,

$$[\mathrm{d}^2k_\perp] = 16\pi^3\delta^2\left(\sum_{i=1}^{n} \boldsymbol{k}_{\perp i}\right) \prod_{i=1}^{n} \frac{\mathrm{d}^2\boldsymbol{k}_{\perp i}}{16\pi^3}\,,$$

and $[\mathrm{d}x]$ denotes integration over the light-cone momentum fractions, i. e.

$$[\mathrm{d}x] = \delta\left(1 - \sum_{i=1}^{n} x_i\right) \prod_{i=1}^{n} \mathrm{d}x_i\,.$$

Let us treat hard exclusive processes in terms of the Brodsky – Lepage approach [11]. In this approach a hard exclusive process involves wave function components with short valence quark separations. In this case, the states that involve only valence quarks determine completely the hadron structure and the distribution function for such processes:

$$\Phi_\lambda^h(x_i, \lambda_i, Q) \propto \int^{k_{\perp i}^2 < Q^2} [\mathrm{d}^2k_\perp]\,\psi_\lambda^h(x_i, \boldsymbol{k}_{\perp i}, \lambda_i)\,. \tag{11}$$

Here $\psi_\lambda^h(x_i, \boldsymbol{k}_{\perp i}, \lambda_i)$ is the valence-quark state amplitude, λ denotes the hadron helicity, and λ_i are the valence quark helicities.

Another important quantity is the scattering amplitude, which relates to the short-distance parton interaction dynamics and can be evaluated perturbatively.

According to the factorisation theorem, the scattering amplitude at the hadron level is the convolution of the distribution functions and the hard scattering amplitude. For the binary process $\mathrm{A} + \mathrm{B} \to \mathrm{C} + \mathrm{D}$, for example,

$$F_{\lambda_\mathrm{A}\lambda_\mathrm{B}\lambda_\mathrm{C}\lambda_\mathrm{D}} = \sum_{\lambda_i} \int [\mathrm{d}x]\,\Phi_{\lambda_\mathrm{C}}^{\mathrm{C}*}(x_i, \lambda_i, Q)\,\Phi_{\lambda_\mathrm{D}}^{\mathrm{D}*}(x_i, \lambda_i, Q)$$
$$\times T_\mathrm{H}(x_i, \lambda_i, Q^2, \theta_{\mathrm{c.m.}})\,\Phi_{\lambda_\mathrm{A}}^{\mathrm{A}}(x_i, \lambda_i, Q)\,\Phi_{\lambda_\mathrm{B}}^{\mathrm{B}}(x_i, \lambda_i, Q)\,, \tag{12}$$

where $[\mathrm{d}x]$ denotes integration over the momentum fractions of partons in the initial and final hadrons, $\mathrm{h} = \mathrm{A, B, C, D}$.

Since the integration over $[\mathrm{d}^2k_\perp]$ in Eqn (11) projects the hadronic wave function on the zero-orbital-momentum $(L_z = 0)$ states, the helicity of the hadron is the sum over the valence quark helicities:

$$\lambda = \sum_{i=1}^{n_h} \lambda_i\,, \tag{13}$$

where n_h is the number of valence quarks in the hadron h. As already mentioned, hard exclusive processes suppress the hadron states which contain some partons in addition to valence quarks.

The hard scattering amplitude T_H conserves quark helicity. This implies the helicity conservation rule

$$\lambda_\mathrm{A} + \lambda_\mathrm{B} = \lambda_\mathrm{C} + \lambda_\mathrm{D}\,. \tag{14}$$

This rule has important experimental implications which are discussed below.

The factorisation theorem and asymptotic freedom also suggest the familiar quark count rule [12]

$$\frac{\mathrm{d}\sigma}{\mathrm{d}t}(\mathrm{A} + \mathrm{B} \to \mathrm{C} + \mathrm{D}) \propto \frac{F(\theta)}{s^{N-2}}\,, \tag{15}$$

where $N = n_\mathrm{A} + n_\mathrm{B} + n_\mathrm{C} + n_\mathrm{D}$. By and large, the rule is in good agreement with the experimental data.

However, for all the apparent simplicity of the problem, difficulties arise in describing hard hadron scattering. For example, Landshoff's [13] disconnected diagrams violate the quark count rule for differential cross sections. The contribution from these diagrams has been examined in detail in Ref. [14].

It is to be noted that in the Brodsky – Lepage approach the hadron and the interaction region are treated as pointlike in nature, whereas the independent quark scattering mechanism implies that they are longitudinally compressed objects, i. e. discs. Since disconnected diagrams correspond to large-transverse-momentum processes, it follows that the emission of gluons by coloured quarks is essential here and leads to inelastic final states.

Thus, these diagrams contribute to inelastic processes, and their contribution to exclusive reactions (in particular to elastic scattering) is suppressed because so are all processes in which the coloured quarks are widely separated and their colour charges do not compensate. Hence contributions to the inelastic scattering may come only from states with short quark separations, when their colour charges mutually compensate and so no gluon emission takes place. As a result, the calculation of the disconnected diagrams including the suppression shows that the decay exponent of the large-angle pp-scattering is 9.59 rather than the quark-count value of 10.

The important point is that the disconnected diagrams conserve quark helicity and that, on the whole, the independent quark scattering mechanism (including the suppression mentioned above) conserves helicity at the hadron level in the s-channel at sufficiently high energies, when the mechanism in question operates at short distances.

Of course, the number of diagrams is huge, and hard scattering amplitudes have not been precisely calculated within the perturbative QCD framework. At present, model approaches are used in quantitatively estimating the perturbative QCD amplitudes and spin – spin correlation parameters such as A_{nn}. In this connection, it is worthwhile to mention the suggestion [15, 16] that the quark exchange diagrams be combined with Landshoff's diagrams in order to describe the experimental behaviour of the spin – spin correlation A_{nn}, one sensitive to the specific form of the helicity amplitudes. We reemphasise, however, that helicity conservation in QCD obtains to all orders in perturbation theoryand for all diagrams independent of their complexity.

Let us next turn to the experimental data, to see how the helicity conservation mentioned above and the power-law prediction for large-angle cross sections are observed. It should be remembered that the power-law cross sections are generally considered as the justification of perturbative QCD in a given kinematic region.

Comparison with experiment shows that power-law differential cross sections are observed at relatively low energies and momentum transfers. For example, for elastic pp-scattering the power law agrees with experimental data starting from $\sqrt{s} = 5$ GeV and $\theta_{\mathrm{c.m.}} \approx 40°$, i.e., for $p_\perp^2 = 2-3$ $(\mathrm{GeV}/c)^2$. This should be remembered when discussing perturbative QCD for quantities associated with the spin degrees of freedom.

The helicity conservation rule (14) gives simple predictions for spin observables in elastic pp-scattering:

$$A = A_{sl} = 0\,, \quad A_{nn} = -A_{ss}\,. \tag{16}$$

Analysing power and spin – spin correlation measurements at large $p_\perp^2$ have been performed in the 10 – 30 GeV range. The measurements show that the relations (16) are not satisfied [3]. The one-spin asymmetry A for $p_{\mathrm{L}} = 28$ GeV/c and large $p_\perp^2$ exhibits a clear tendency to rise with $p_\perp^2$ and reaches 24% for $p_\perp^2 = 6.5$ $(\mathrm{GeV}/c)^2$ (see Fig. 2). The parameter A_{nn} reaches 60% at $\theta_{\mathrm{c.m.}} = 90°$ and $p_{\mathrm{L}} = 12$ GeV/c. This implies the following cross-section ratio for proton interactions with parallel and antiparallel spins (see Fig. 1):

$$\frac{\mathrm{d}\sigma/\,\mathrm{d}t|_{\uparrow\uparrow}}{\mathrm{d}\sigma/\,\mathrm{d}t|_{\uparrow\downarrow}} = 4\,. \tag{17}$$

This value cannot be obtained from diagrammatical perturbative QCD models. If the above discrepancies between perturbative QCD and experiment persist into higher energies, this will be strong evidence for the nonperturbative nature of the spin effect dynamics.

3. Nonperturbative approaches to spin effects in elastic scattering

Let us consider some of the nonperturbative approaches to the understanding of spin effects in elastic scattering. In addition to being asymptotically free, QCD must also predict two nonperturbative phenomena: confinement and chiral symmetry breaking. The corresponding scales are characterised by the parameters Λ_{QCD} and Λ_χ, respectively [17]: $\Lambda_{\mathrm{QCD}} = 100-300$ MeV, $\Lambda_\chi \approx 4\pi f_\pi \approx 1$ GeV, where f_π is the pion decay coupling constant. The chiral $\mathrm{SU}(3)_{\mathrm{L}} \times SU(3)_{\mathrm{R}}$ symmetry is broken spontaneously at distances in between these scales. The chiral symmetry breaking mechanism leads to quark mass production, with the quarks acquiring an internal structure as a result [17]. These nonperturbative features are both being invoked for explaining the observed spin effects. We shall consider the confinement-involving approaches first.

3.1 Quark confinement and spin effects

3.1.1 Resonance amplitude contribution To describe the observed behaviour of A_{nn}, the pp-scattering amplitude at 12 GeV/c was assumed [18] to have a contribution from the s-channel resonance structure (R) related to the excitation of the 'latent flavour' $|\mathrm{qqqqqqQQ}\rangle$ in colour-singlet channels at the strange- and charmed-quark production thresholds. The model amplitude consists of the perturbative QCD part (background term) and the resonance amplitude:

$$F_i = F_i^{\mathrm{q}} + F_i^{\mathrm{R}}\,. \tag{18}$$

The resonance amplitudes account for the large-distance contribution, i. e. the confinement effect. Eqn (18) represents an attempt to go beyond perturbative QCD.

As background amplitudes, quark-exchange amplitudes have been chosen, these being dominant over their quark-annihilation and gluon-exchange counterparts in exclusive two-particle processes. Quark exchange amplitudes give a value $A_{nn} = 1/3$, virtually independent of the energy and the scattering angle. Consequently, these amplitudes fail to describe the experimental data [3].

The resonance contributions F_i^{R} are of the Breit – Wigner form, and for $J = L = S = 1$ the two nonzero helicity amplitudes may be represented as

$$F_{3,4}^{\mathrm{R}} = \pm 12\pi \frac{\sqrt{s}}{p_{\mathrm{c.m.}}} d^{\,1}_{\pm 1,1}(\theta_{\mathrm{c.m.}}) \frac{1/2\Gamma^{\mathrm{pp}}(s)}{M^* - E_{\mathrm{c.m.}} - \mathrm{i}/2\Gamma}\,. \tag{19}$$

According to the basic assumption about the structure of a resonance with baryon number of $B = 2$, it is expected that Eqn (19) must have contributions from states with masses $M = 2.55$ and 5.08 GeV, these masses corresponding to the open-strangeness ($\mathrm{pp} \to \Lambda\mathrm{K}^+\mathrm{p}$) and open-charm ($\mathrm{pp} \to \Lambda_{\mathrm{c}}\mathrm{D}^0\mathrm{p}$) threshold values.

While this scheme does account for the behaviour of a spin – spin correlation parameter (Fig. 4), the absence of a single-helicity-change amplitude ($F_5 = 0$) leads to a nonzero one-spin asymmetry A.

Without expanding on this here we mention only that there are a number of other schemes for going beyond perturbative QCD to explain spin effects, some of these involving diquarks [19], pinch singularity contributions [20], preasymptotic effects [21], and interaction geometry [22]. The basic assumptions and main results of these models are summarised in Table 1.

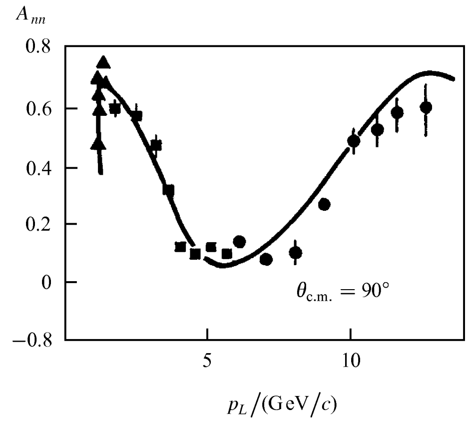

Figure 4. Parameter A_{nn} in the latent flavour model [18].

Table 1.

Model	Dynamical assumptions	Results
Diquarks	Diquarks as components of the nucleonic wave function	Nonzero helicity-flip amplitude F_5, behaviour of the analysing power
Pinch singularities	Dominant role of leading ($x \to 1$) quarks in scattering processes	Behaviour of the parameters $A_{nn}(90°)$ and $A_{ll}(90°)$
Preasymptotic effects	Soft rescattering in initial and final states, quasipotential equation for the amplitude	γ_5-invariance violation at finite energies, behaviour of the parameter A_{nn}, polarisation decaying with energy as $1/s$
Geometrical picture	Eikonal representation for the central, spin – orbit, and spin – spin interactions	Rise in A_{nn} due to the spin – spin interaction being more peripheral than the spin – orbit interaction

3.1.2 Massive quark model The massive quark model is based on the so-called quantum geometrodynamics concept [23]. Quantum geometrodynamics includes quark confinement directly: the quark propagator is free of singularities. Quark spectators conserve their spins. The elementary quark – quark amplitude

$$\mathrm{qq} \to \mathrm{qq}$$

is determined by summing an infinite number of meson exchanges which include not only transverse vector states (analogous to gluons) but also longitudinal vector and pseudoscalar configurations of quarks and antiquarks. As a result, the qq-scattering amplitude

$$F_{\{\lambda_i\}} = F^{V_\mathrm{T}}_{\{\lambda_i\}} + F^{V_\mathrm{L}}_{\{\lambda_i\}} + F^{P}_{\{\lambda_i\}} \tag{20}$$

has a rich spin structure in the region of large angles.

In this approach the helicity amplitudes at the hadron level are all nonzero; for example, for pp scattering we have $F_i \neq 0$. However, the BB scattering amplitudes are real functions and hence the analysing power is zero because of the lack of phase difference between the helicity amplitudes. It has therefore been suggested [24] that, for large scattering angles, the contribution from the helicity-conserving imaginary diffraction amplitude be added, with the possibility of an appreciable interference effect. As a result, the analysing power A at 28 GeV/c increased up to 33%, to be compared with the experimental value of 24% (see Fig. 5). For much larger values of $p_\perp^2$, A decreases rapidly. The parameter A_{nn} at 28 and 50 GeV/c increases with scattering angle, approaching unity at 90°.

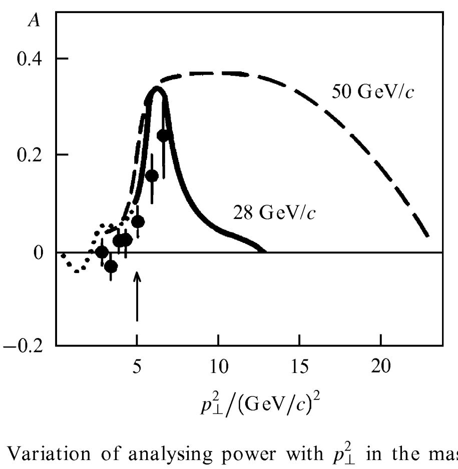

Figure 5. Variation of analysing power with $p_\perp^2$ in the massive quark model [24].

3.2 Spontaneous breaking of chiral symmetry, and hadron scattering

In order to explain the behaviour of spin observables, it seems reasonable to invoke ideas involving the spontaneous breaking of the chiral symmetry. Because of this breaking, the hadron structure differs from the parton model even at distances of a few tenths of a fermi. In particular, the breaking of the chiral symmetry yields quark masses comparable with the hadron mass scale. So at large distances a hadron appears as a loosely bound system of its constituent quarks. This view of hadron structure has provided an understanding of some features seen in hadron interactions at large distances. In particular, this yields fairly reasonable values for statistical hadron characteristics such as, for example, magnetic moments [25].

It should be emphasised that large spin effects long observed in hard processes indicate that hadron interaction dynamics is of a nonperturbative nature even at short distances. Further confirmation of this is found in the study of hadron structure in deep-inelastic scattering. It has been found [26] that chiral models give a lucid explanation of the spin structure function $g_1(x)$ measured in the deep-inelastic scattering of polarised muons on a polarised proton target.

The success of the chiral-symmetry-breaking models naturally leads to attempts at their extension, in particular to include hadron interactions at short distances. Some of the ideas of the chiral models have been applied [27] to the description of hadron scattering in a unified fashion at both large and short distances [28].

3.2.1 Nonperturbative hadron structure Most hadron interactions take place at distances at which the chiral symmetry breaks spontaneously. Since this distance is less than the confinement radius, a description in terms of constituent quarks is adequate for the problem under study.

Some of the effective-Lagrangian models (see, for example, Ref. [29]) describe hadron structure by including the spontaneous breaking of the chiral symmetry. Since effective Lagrangians presumably describe the nonperturbative QCD properties (in the limit $N_\mathrm{c} \to \infty$, for example), it is believed that such models provide the realisation of these properties. For a survey of chiral models see Ref. [30]. As a starting point in discussing hadron structure and hadron interaction dynamics we choose two models: the modified versions of the σ model [31] and of the Nambu – Jona – Lasinio (NJL) model [32].

We first note that most chiral models represent a baryon as consisting of an inner core region carrying a baryon charge, and an external cloud around the core. The existence of the core region is suggested by data both for low [33] and for high [34, 35] energies. In particular, the $p_\perp$ distribution of muon pairs at large masses may be explained by the assumption that the central part of the proton consists of valence quarks and has a radius of 0.20 ± 0.03 fermi. A phenomenological analysis of elastic scattering data also suggests the presence of a central region within the proton [35].

In the modified σ model massless quarks interact with a boson field, whereas the NJL model involves a nonlinear four-fermion interaction. The former model employs a local-gauge-invariant $SU(3)_L \times SU(3)_R$ symmetric scheme. The cloud of interacting quarks appears in the outer region of the soliton that arises in a nonlinear σ model. The quark interaction is realised by means of the scalar field as follows:

$$-g\xi(x)\left[\bar{\psi}_L(x)\psi_R(x) + \bar{\psi}_R(x)\psi_L(x)\right] . \tag{21}$$

The scalar field $\xi(x)$ is a nonzero function outside the soliton.

Because of the interaction, massless quarks may form zero-momentum zero-spin states, and the quark system may go over into a new ground state, one containing a quark condensate. This mechanism was originally suggested [32] by invoking the superconductivity analogy. The new ground state is a superposition of quark pair states. The quark condensate concept and the notion of a quark-condensate-containing hadron have been introduced on the basis of on the NJL model. Originally this model assumed nucleon fields to be fundamental ones. With the advent of QCD, a quark field reformulation of the model was developed.

The starting point is the nonlinear four-fermion Lagrangian

$$L = \bar{\psi} i\gamma^\mu \partial_\mu \psi + \tfrac{1}{2} g^2 [(\bar{\psi}\boldsymbol{\tau}\psi)^2 - (\bar{\psi}\gamma_5\boldsymbol{\tau}\psi)^2] , \tag{22}$$

where g is a coupling constant with the dimensions of length, and $\boldsymbol{\tau}$ represents the isospin matrix. This Lagrangian is invariant under chiral transformations,

$$\psi(x) \to \exp\{i\gamma_5 \boldsymbol{\tau\alpha}\}\psi(x) ,$$
$$\bar{\psi}(x) \to \bar{\psi}(x) \exp\{i\gamma_5 \boldsymbol{\tau\alpha}\} .$$

Expression (22) may be considered as the simplest possible effective Lagrangian capable of reflecting the basic nonperturbative features of QCD. It has been demonstrated that the chiral symmetry is broken dynamically, and a quark acquires mass, as the coupling constant g increases beyond a certain critical value. Thus, the interaction of massless fermions generates the dynamical mass of the quark. In this approach a massive quark appears as a quark condensate excitation and may be regarded as a quasiparticle (a mixture of right and left quarks).

It is reasonable to assume that as a result of the breaking of the chiral symmetry, in addition to the mass

$$m_q \propto -\frac{1}{\Lambda_\chi^2}\langle\bar{\psi}\psi\rangle , \tag{23}$$

the quark acquires a certain internal structure and a final size. The quark radius r_q also must be related to the order parameter $\langle\bar{\psi}\psi\rangle$ and hence to the mass:

$$r_q \propto \frac{1}{m_q} . \tag{24}$$

Originally this relation was introduced phenomenologically in the analysis of elastic scattering data [36]. Relation (24) was shown to yield correct values for total cross section ratios for various hadron reactions. Later a similar quark radius expression was obtained within the NJL model [37].

Based on the results above, the hadron may naturally be thought to consist of an inner region (the location of the valence quarks), and a condensate-filled outer region. The valence quarks then appear as extended objects. They are described by their size and by the distribution of quark matter.

3.2.2 Elastic hadron scattering model In this case the first stage in a hadron collision event involves the overlapping of hadron structures and the interaction of the condensates. The excitation of a condensate in the overlap region gives rise to quasiparticles, that is, to massive quarks. The number of these is estimated by assuming that some of the energy carried by the outer clouds is released in the overlap region to be expended on massive quark formation. The number of quarks produced in a hadron collision is then estimated to be

$$\tilde{N}(s,b) \propto \frac{(1-k)\sqrt{s}}{m_q} D_c^A \otimes D_c^B , \tag{25}$$

where m_q is the quark mass and k is the fraction of energy corresponding to the valence quarks.

The function D_c^H describes the distribution of the condensate within the hadron H, and b is the impact parameter of the colliding hadrons A and B. Thus, $\tilde{N}(s,b)$ virtual quarks appear in addition to N valence quarks ($N = n_A + n_B$). In elastic scattering the quarks produced transform into the condensates of scattered hadrons at the final stage of the interaction.

The model rests on the assumption that valence quarks are scattered quasi-independently by a certain external field which is produced by the virtual quarks and by the self-consistent field of the quarks themselves. In conformity with the quasi-independent nature of the valence quarks, the initial form of the principal dynamic quantity employed may be given by the following product (in the impact parameter representation [38]):

$$U(s,b) = \prod_{q=1}^{N} f_q(s,b) . \tag{26}$$

The factors $f_q(s,b)$ correspond to the scattering amplitudes of individual valence quarks in the effective field which is produced by the virtual and valence quarks.

The function $U(s,b)$ represents the generalised reaction matrix. The scattering amplitude F is related to the function U by (see Ref. [39])

$$F = U + i\int d\Omega\, UF . \tag{27}$$

This relation secures the unitarity condition, provided

$$\operatorname{Im} U(s,b) \geqslant 0 . \tag{28}$$

Implications of the scattering amplitude being unitarised by means of the generalised reaction matrix are discussed in Ref. [28].

In accordance with the idea of quarks being scattered in an effective field, $f_q(s,b)$ is written in the form

$$f_q(s,b) = [\tilde{N}(s,b) + N - 1]V_q(b) , \tag{29}$$

where the function $V_q(b)$ may be represented as a convolution,

$$V_q(\boldsymbol{r}) = \int D_q(\boldsymbol{r}_1) v_{qq}(\boldsymbol{r}+\boldsymbol{r}_1-\boldsymbol{r}_2) D_q(\boldsymbol{r}_2)\,\mathrm{d}^3\boldsymbol{r}_1\,\mathrm{d}^3\boldsymbol{r}_2\ , \qquad (30)$$

$$V_q(b) = \int_{-\infty}^{\infty} V_q\left(\sqrt{|\boldsymbol{b}|^2+z^2}\right)\mathrm{d}z\ . \qquad (31)$$

In Eqn (30) the function v_{qq} describes the quark–quark interaction, $D_q(\boldsymbol{r})$ is the quark distribution function, and $\boldsymbol{r}_1$ and $\boldsymbol{r}_2$ are the quark-centre coordinates. It is understood that the longitudinal degrees of freedom of the quarks have been integrated out.

As already stated, a massive quark is a quasiparticle, i.e. a mixture of right and left quarks which interact contact-wise in the NJL model. It is therefore quite natural to relate the quark interaction radius to the quark size and to take the interaction amplitude to be proportional to the convolution of the quark matter densities:

$$v_{qq} \propto d_q \otimes d_q\ , \qquad (32)$$

where d_q is the quark matter distribution function within the massive quark.

Taking for this distribution (or the quark form factor) the simple exponential form $d_q \propto \exp(-r/r_q)$ we obtain

$$v_{qq} \propto \exp(-r/r_q)\ . \qquad (33)$$

Then from Eqns (30) and (33) the function $V_q(b)$ follows as

$$V_q(b) \propto \exp(-m_q b)\ . \qquad (34)$$

The explicit expression for $V_q(b)$ has been obtained under certain simplifying assumptions. The function $V_q(b)$ may be more complex in form because of a more complicated v_{qq} dependence or because the distribution function $D_q(r)$ may fall off less rapidly. While the inclusion of these factors is important for fitting the data quantitatively, for qualitative purposes the expressions above will do.

Note that because of the peripheral nature of the condensate distribution within a hadron the dependence of the convolution $D_\mathrm{c} \otimes D_\mathrm{c}$ on the impact parameter is weak compared to the function $V_q(b)$ and may therefore be neglected.

We now turn to consider the spin structure of the hadron and the spin dependence of hadron interactions. In the approach being considered a quark is an extended entity having an inner structure. So it is natural to relate the quark spin to the orbital motion of the quark matter. It is precisely in this way that spin is treated in the effective-Lagrangian approach [26, 29].

A change in quark helicity may occur via the interaction of a valence quark with a virtual one. Virtual quarks differ in helicity, so that an exchange process involving a valence quark and its virtual counterpart with opposite helicity (but with the same flavour) will secure a necessary change in quark helicity,

$$\mathrm{q}_+ \to \mathrm{q}_-\ .$$

Based on the NJL model, it is assumed that the qq interaction is one of a contact type.

Let us introduce two functions describing the helicity-flip and helicity-conserving scattering of a quark in the effective field. The choice of these is based on the above interaction picture:

$$f_q(s,b) = g_q(s)\exp\left[-m_q b + \mathrm{i}\phi_q(s)\right]\ ,$$

$$f_{qf}(s,b) = g_{qf}(s)\exp\left[-\alpha m_q b + \mathrm{i}\phi_{qf}(s)\right]\ . \qquad (35)$$

The quark exchange process plays a more critical role than does quark scattering. In fact, a valence quark 'knocks out' a corresponding quark with opposite helicity but with the same flavour. Such an interaction must be more important, and is less likely due to the effectively reduced number of participating quarks relative to elastic scattering. This gives the following intensity ratio for helicity-flip and helicity-nonflip quark scattering in the effective field:

$$\frac{g_q(s)}{g_{qf}(s)} \propto N_q(s)\ . \qquad (36)$$

Eqn (36) gives the suppression of the helicity-flip relative to the helicity-nonflip scattering.

Naturally, the amplitudes (35) have different phases. In the optical picture the phase may be related to the number of scattering particles. We therefore assume that the difference in phase between the helicity amplitudes has the following dependence:

$$\Delta(s) = \phi_q(s) - \phi_{qf}(s) \propto N_q(s)\ . \qquad (37)$$

Thus, in the analysis of experimental data on $\Delta(s)$ a two-parameter linear function of $\sqrt{s}$ is employed.

Note that there exist hierarchical relations between the ratios of the single- and double-helicity-flip functions to the nonflip function:

$$\frac{U_5(s,b)}{U_1(s,b)} \propto \frac{m_q}{\sqrt{s}}\ , \quad \frac{U_2(s,b)}{U_1(s,b)} \propto \frac{m_q^2}{s}\ . \qquad (38)$$

These relations are at first sight reminiscent of perturbative QCD. There are, however, three points of distinction which should be mentioned.

First, we are discussing a nonperturbative approach and hence Eqn (38) does not involve a factor α_s, and the mass m_q is that of a constituent quark and so is of the order of the hadron mass. This last circumstance is a consequence of the breaking of the chiral symmetry. Second, relations (38) hold for functions as taken in the impact parameter representation. Finally, these relations are not for amplitudes but rather for the U matrix, further to be subjected to a unitarisation procedure.

As we shall see, the above features lead to a considerable difference in the behaviour of spin dependent observables.

3.2.3 Helicity amplitudes in hadron scattering The analytical evaluation of scattering amplitudes involves the analysis of singularities in the complex impact-parameter plane [40, 41].

In order to carry out an analytical calculation of the five helicity amplitudes of the pp scattering, $F_i(s,t)$, $i = 1, 2, \ldots, 5$, the corresponding amplitudes in the impact parameter representation, $f_i(s,\beta)$, $\beta = b^2$, are continued into the complex β plane and the integral over the impact parameter is transformed into one along the contour C around the positive half-axis. We then have the following representations for the helicity amplitudes:

$$F_i(s,t) = -\frac{is}{2\pi^3}\int_C d\beta\, f_i(s,\beta)K_0(\sqrt{t\beta}), \quad t<0, \quad i=1,2,3,$$

$$F_4(s,t) = \frac{is}{2\pi^3}\int_C d\beta\, f_4(s,\beta)K_2(\sqrt{t\beta}), \tag{39}$$

$$F_5(s,t) = -\frac{is}{4\pi^3}\sqrt{-t}\int_C d\beta\,\sqrt{\beta}f_5(s,\beta)[K_0(\sqrt{t\beta})-K_2(\sqrt{t\beta})],$$

where the $K_j(x)$ are modified Bessel functions.

The amplitudes $f_i(s,\beta)$ have poles in the complex β plane whose positions are determined by the zeros of the denominator in the appropriate unitarised U-matrix representa-tion [39]:

$$\beta_n(s) = \frac{1}{M^2}\ln\left[\tilde{g}\left(\frac{s}{m_q^2}\right)^{N/2}\right] + i\pi n, \quad n=\pm 1, \pm 3, \ldots, \tag{40}$$

where $M = m_q N$ and $\tilde{g}$ is a constant. The helicity amplitudes $f_i(s,\beta)$ have a branch point at $\beta = 0$ in addition to the poles.

Thus, the helicity amplitudes can be represented as a sum of the contribution from the poles and that from the cut:

$$F_i(s,t) = F_{i,\mathrm{p}}(s,t) + F_{i,\mathrm{c}}(s,t). \tag{41}$$

Note that these contributions are dynamically separable since $g_q(s) \to \infty$ as $s \to \infty$. This behaviour of the function $g_q(s)$ corresponds to the asymptotical rise in total cross sections.

The contributions from the poles in the complex impact-parameter plane determine the behaviour of the amplitude in the region $|t|/s \ll 1$ ($t \neq 0$). The helicity parameters can be represented as a series in the parameter $\tau(\sqrt{-t})$,

$$F_i(s,t) = s\sum_{k=1}^{\infty}\tau^k(\sqrt{-t})\Phi_k^{(i)}\left[R(s),\sqrt{-t}\right], \tag{42}$$

where the functions $\Phi_k^{(i)}[R(s), \sqrt{-t}\,]$ oscillate in the variable $\sqrt{-t}$ and τ decreases exponentially with it:

$$\tau(\sqrt{-t}) = \exp\left(-\frac{\pi}{M}\sqrt{-t}\right). \tag{43}$$

For intermediate values of t we need keep only a few or even one term in the series for the helicity amplitude. The differential cross section in this region exhibits the Orear behaviour:

$$\frac{d\sigma}{dt} \propto \exp\left(-\frac{2\pi}{M}\sqrt{-t}\right). \tag{44}$$

This is in agreement with experiment giving an estimated quark mass of $m_q \approx 200$ MeV. In this region the analysing power has an oscillatory dependence on the momentum transfer.

The period of the oscillations is determined by the effective interaction radius, which grows logarithmically as $s \to \infty$:

$$R(s) = \frac{N}{2M}\ln s. \tag{45}$$

Thus, for scattering in the region $|t| \ll s$ the one-spin asymmetry oscillations are determined by the contributions from the poles in the complex impact-parameter plane and are a consequence of the unitary condition in the direct reaction channel.

The large-angle behaviour of the helicity amplitude $F_i(s,t)$ ($s \to \infty$, with $|t|/s$ fixed) is determined by the contribution from the cut $\beta \in [0, -\infty)$:

$$F_i(s,t) = \frac{s}{\pi^3}\int_{-\infty}^{0} d\beta\,\mathrm{disc}f_i(s,\beta)K_0(\sqrt{t\beta}), \quad i=1,2,3,$$

$$F_4(s,t) = -\frac{s}{\pi^3}\int_{-\infty}^{0} d\beta\,\mathrm{disc}f_4(s,\beta)K_2(\sqrt{t\beta}), \tag{46}$$

$$F_5(s,t) = -\frac{s}{\pi^3}\int_{-\infty}^{0} d\beta\,\mathrm{disc}f_5(s,\beta)K_1(\sqrt{t\beta}).$$

Performing the integrals and taking into account the particle identity we are led to the following expressions for the helicity amplitudes in wide-angle pp scattering:

$$F_1(s,\theta) = \omega(s)M\left(|t|^{-3/2} + |u|^{-3/2}\right),$$

$$F_2(s,\theta) = -\omega(s)\tilde{M}_f\left[\frac{g_{qf}(s)}{g_q(s)}\right]^2\exp[-2i\Delta(s)](|t|^{-3/2} + |u|^{-3/2}),$$

$$F_3(s,\theta) = \omega(s)\left\{M|t|^{-3/2} - 3\tilde{M}_f\left[\frac{g_{qf}(s)}{g_q(s)}\right]^2\exp[-2i\Delta(s)]|u|^{-3/2}\right\},$$

$$F_4(s,\theta) = -F_3(s,\pi-\theta), \tag{47}$$

$$F_5(s,\theta) = \omega(s)\frac{g_{qf}(s)}{g_q(s)}\exp[-i\Delta(s)]\left(|t|^{-3/2} + |u|^{-3/2}\right),$$

where

$$\omega(s) = \frac{s}{\pi^2 g_q^N(s)}\exp[-iN\phi_q(s)], \quad \tilde{M}_f = M + 2m_q(1-\alpha).$$

For large momentum transfers ($s \to \infty$, $|t|/s$ fixed), the contribution from the branch point ($\beta = 0$) dominates. The angular distribution here has the following power-law dependence:

$$\frac{d\sigma}{dt} \propto \left(\frac{1}{s}\right)^{N+3} f(\theta). \tag{48}$$

Superimposed on the power-law dependence are oscilla-tions whose explicit form is omitted here. The behaviour (48) is consistent with the data, although the values of the exponent are somewhat different from those originally obtained by the quark count rule and later derived within the perturbative QCD framework. The discrepancy is due to there being a mass scale of the order of the hadron mass in the model.

As noted earlier, this mass is due to the spontaneous breaking of the chiral symmetry. In this sense the above model is close to the mechanism of Landshoff [13] which also deviates from the quark count rule because of a mass scale present in the problem. Further common features may be found if one notices that quark scattering is independent in both models.

3.3 Analysing power and spin–spin correlation parameters

Explicit expressions for the helicity amplitudes allow certain conclusions to be drawn concerning the behaviour of spin observables at large scattering angles. It is in this way that nonzero one-spin asymmetry was predicted [42]. For large-angle pp scattering the analysing power behaves as follows:

$$A(s,\theta) = -\frac{4\sin\Delta(s)}{(1-k)N}f(\theta)\left[1 + O\left(\frac{m_q^2}{s}\right)\right], \tag{49}$$

where

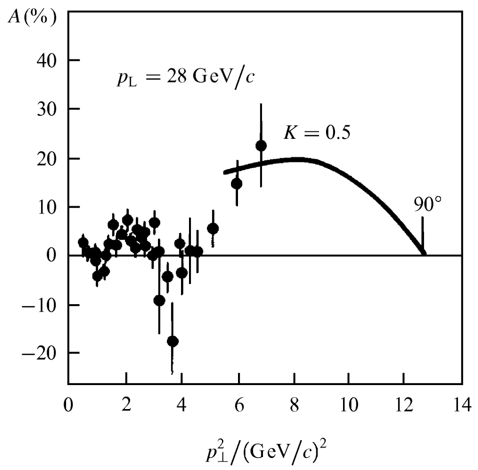

Figure 6. Analysing power at large angles in the U-matrix model.

$$f(\theta) = \frac{\sin 2\theta\left[\cos^3(\theta/2) + \sin^3(\theta/2)\right]}{3\cos 2\theta + 5 + \sin^3\theta + (1-k)^{-2}N^2\sin^2\theta} \, .$$

Usually the parameter k is taken to be 1/2, implying that half of the hadron energy is carried by the valence quarks. Fig. 6 compares experimental data with the corresponding expression for the analysing power A.

In the case of πN scattering the analysing power is

$$A(s,\theta) = -\frac{2\sin\Delta(s)}{(1-k)N}\,\frac{\sin(\theta/2)}{1+(1-k)^{-2}N^{-2}\sin^2(\theta/2)} \times\left[1+\mathrm{O}\left(\frac{m_q^2}{s}\right)\right] . \qquad (50)$$

In the region of large angles $A(s,\theta)$ may be as high as 60%.

It has also been predicted that the analysing power is an oscillatory function of s because the energy dependence of this quantity is determined by the phase difference $\Delta(s)$. From the optical picture of valence quark scattering in the effective field it follows that the phase difference $\Delta(s)$ increases with energy. The one-spin asymmetry remains nonzero at the asymptotic energies and hence is amenable to observation at very high energies. The experimental test of this prediction is crucial for the model.

The spin – spin correlation expressions for elastic pp scattering through a (centre-of-mass) angle $\theta_{\mathrm{c.m.}} = 90°$ are

$$A_{nn}(s,90°) = \frac{1}{3}\left\{1 - \frac{8m_q^2}{(1-k)^2 s}\left[1+\frac{2}{N}(1-\alpha)\right]\cos 2\Delta(s)\right\} ,$$

$$A_{ll}(s,90°) = -\frac{1}{3}\left\{1 + \frac{8m_q^2}{(1-k)^2 s}\left[1+\frac{2}{N}(1-\alpha)\right]\cos 2\Delta(s)\right\},$$

$$A_{ss}(s,90°) = -\frac{1}{3} + \mathrm{O}\left(\frac{m_q^4}{s^2}\right). \qquad (51)$$

The explicit expression for the differential cross section is

$$\frac{\mathrm{d}\sigma}{\mathrm{d}t}(s,90°) = \sigma_0(s)\left\{1 - \frac{2m_q^2}{(1-k)^2 s}\left[1+\frac{2}{N}(1-\alpha)\right]\cos 2\Delta(s)\right\}, \qquad (52)$$

where

$$\sigma_0(s) \propto \left(\frac{1}{s}\right)^{N+3} .$$

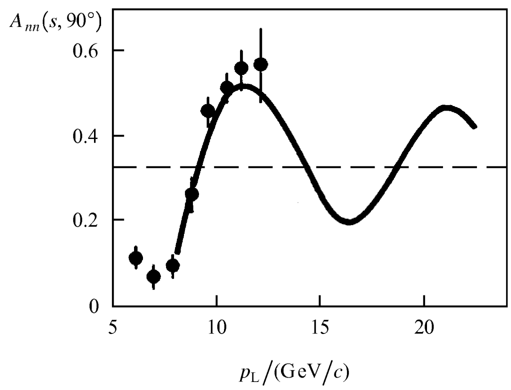

Figure 7. Comparison of the quark U matrix model and experimental data for $A_{nn}(s, 90°)$.

It is readily seen that the power-law behaviour of the cross section is modified by superimposed oscillations. These latter have indeed been observed experimentally in large-angle cross section measurements (see, for example, Ref. [43]). The behaviour of the spin – spin correlation parameters as a function of the energy is also oscillatory in character. This behaviour explains the observed energy dependence of the parameter $A_{nn}(s, 90°)$ in the interval $p_L = 6-12$ GeV/c (Fig. 7).

The helicity amplitude expressions (47) yield spin – spin correlation parameters for any scattering angles. Thus, for the parameter A_{nn} for $p_L = 18.5$ GeV/c and $p_\perp^2 = 4.7\ (\mathrm{GeV}/c)^2$, we have $A_{nn} = -6\%$. All the above results are in agreement with the experimental data.

The oscillations in s are a consequence of the optical approach to valence quark scattering. The quark condensate appears as a result of the spontaneous breaking of the chiral symmetry. The internal quark structure which results is characterised by a finite (r_q-dependent) size and a certain distribution of the quark matter (quark form factor).

Based as it is on the nonperturbative dynamics properties mentioned above, the model described is capable of predicting the main features of elastic scattering for any values of momentum transfer, as well as accounting for spin effects. It is to be emphasised that the power-law behaviour of the large-angle differential cross sections can also be obtained nonperturbatively.

This last circumstance implies however that the power-law hard-scattering cross sections are not by themselves sufficient to justify perturbative QCD. For this, at least one more condition must be met — that one-spin transverse asymmetries be vanishingly small in the hard region. There is at present no such tendency experimentally.

In considering the hadron structure and hadron interaction dynamics we relied upon the results obtained from the models involving spontaneously broken chiral symmetry. The unitarity property in the direct channel of a reaction was accounted for explicitly and it was demonstrated that both short- and long-distance hadron interactions may be treated within a single framework.

It should be emphasised that the measurement of the analysing power and spin – spin correlation in elastic scattering provides an explicit and unambiguous way of testing both perturbative QCD itself and models that use nonperturbative approaches to hadron dynamics.

4. Inclusive processes and spin effects

We next address ourselves to spin effects in inclusive reactions and consider problems amenable to study by means of accelerated, polarised proton beams. Measurements of spin observables in collisions of a polarised proton beam with unpolarised antiprotons in, for example, the FNAL collider, are expected to give an independent check of the standard model, including the strong interaction sector, QCD.

4.1 Implications of perturbative quantum chromodynamics

Consider a polarised beam reaction

$$\mathrm{A}_{\uparrow} + \mathrm{B} \to \mathrm{C} + \mathrm{X} , \tag{53}$$

when the hadron A is polarised transversely (N) or longitudinally (L) relative to the momentum. The simplest observable quantity is the one-spin asymmetry A defined by analogy with the analysing power for binary reactions as

$$A = \frac{E_C\,\mathrm{d}\sigma/\,\mathrm{d}^3 p_C|_{\uparrow} - E_C\,\mathrm{d}\sigma/\,\mathrm{d}^3 p_C|_{\downarrow}}{E_C\,\mathrm{d}\sigma/\,\mathrm{d}^3 p_C|_{\uparrow} + E_C\,\mathrm{d}\sigma/\,\mathrm{d}^3 p_C|_{\downarrow}} . \tag{54}$$

From the parity conservation in strong interactions, only the transverse asymmetry A_{N} may be different from zero in reactions (53). An observation of nonzero longitudinal asymmetry A_{L} in hadron processes would indicate the presence of a parity-breaking term in strong interactions. However in electroweak interactions, where parity is not conserved, the helicity (or longitudinal) asymmetry A_{L} may also differ from zero.

Although in the processes under consideration only one of the colliding hadrons is polarised, it should be noted that such reactions also enable two-spin asymmetries to be measured. Thus, the polarisation of unstable particles in their final state may be measured from the angular distribution of decay products (Λ hyperon, for example).

Thus, for the initial hadron A polarised longitudinally, the asymmetry transfer, D_{LL}, can be measured by observing the longitudinal polarisation C of the final particle:

$$D_{\mathrm{LL}} = \frac{E_C\,\mathrm{d}\sigma/\,\mathrm{d}^3 p_C|_{\rightrightarrows} - E_C\,\mathrm{d}\sigma/\,\mathrm{d}^3 p_C|_{\rightleftarrows}}{E_C\,\mathrm{d}\sigma/\,\mathrm{d}^3 p_C|_{\rightrightarrows} + E_C\,\mathrm{d}\sigma/\,\mathrm{d}^3 p_C|_{\rightleftarrows}} . \tag{55}$$

The arguments presented hold, naturally, for the case of transverse asymmetries as well.

We consider one-spin asymmetries first. The QCD factorisation theorem enables the inclusive cross section to be presented as an incoherent sum over the cross sections of all possible hard subprocesses [11]:

$$\begin{aligned} E_C \frac{\mathrm{d}\sigma}{\mathrm{d}^3 p_C}(\lambda_{\mathrm{a}}, \lambda_{\mathrm{b}}, \lambda_{\mathrm{c}}) &= \sum_{\lambda_{\mathrm{a}},\lambda_{\mathrm{b}},\lambda_{\mathrm{c}},\lambda_{\mathrm{d}}} \int_0^1 \mathrm{d}x_{\mathrm{a}} \int_0^1 \mathrm{d}x_{\mathrm{b}} \int_0^1 \mathrm{d}x_{\mathrm{c}}\,\frac{1}{x_{\mathrm{c}}} \\ &\times G^{\mathrm{a}}_{\mathrm{A},\lambda_{\mathrm{A}}}(x_{\mathrm{a}}, \lambda_{\mathrm{a}}, Q) G^{\mathrm{b}}_{\mathrm{B},\lambda_{\mathrm{B}}}(x_{\mathrm{b}}, \lambda_{\mathrm{b}}, Q) D^{\mathrm{C},\lambda_{\mathrm{C}}}_{\mathrm{c}}(x_{\mathrm{c}}, \lambda_{\mathrm{c}}, Q) \\ &\times \delta(s' + t' + u')\frac{s'}{\pi}\,\frac{\mathrm{d}\sigma^{\mathrm{ab}\to\mathrm{cd}}}{\mathrm{d}t'}(\lambda_{\mathrm{a}}, \lambda_{\mathrm{b}}, \lambda_{\mathrm{c}}, \lambda_{\mathrm{d}}) , \end{aligned} \tag{56}$$

where λ_{A} and λ_{a} are the helicities of hadron A and parton a, respectively; G denotes the structure function and D, the fragmentation function.

The quark and gluon structure functions are related to the light-cone wave functions by

$$G^{\mathrm{a}}_{\mathrm{A},\lambda_{\mathrm{A}}}(x, \lambda, Q) \propto \sum_{n,\lambda_i} \int^{Q} [\mathrm{d}^2 k_{\perp}][\mathrm{d}x] |\psi_n(x_i, \lambda_i, k_{\perp,i}|^2 \delta(x - x_{\mathrm{a}}) . \tag{57}$$

The structure functions are nonperturbative entities, and it is the important task of spin studies to determine the dependence of the probability $|\psi_n(x_i, \lambda_i, k_{\perp,i})|^2$ on the number, type, and helicity of the constituents.

Now Fock states with any number of quarks and gluons and with arbitrary orbital momenta contribute to the structure function G. Thus the sum over the helicities of all the constituents is not equal to the hadron helicity λ_{H}. The only relation available is

$$\lambda_{\mathrm{H}} = \lambda_{\mathrm{q}} + \lambda_{\mathrm{g}} + \langle L_z \rangle_{\mathrm{q}} + \langle L_z \rangle_{\mathrm{g}} ,$$

where λ_{q} and λ_{g} represent the total quark and gluon helicities and $\langle L_z \rangle_{\mathrm{q}}$ and $\langle L_z \rangle_{\mathrm{g}}$ are the corresponding orbital angular momenta.

Given the structure functions, the factorisation theorem allows us to calculate the cross sections of hard processes and the corresponding two- and one-spin asymmetries by suggesting the following expression for the cross section difference:

$$\Delta\sigma^{\mathrm{A+B\to C+X}} = \sum_{\mathrm{a,b,c,d}} \int \Delta G^{\mathrm{a}}_{\mathrm{A}} G^{\mathrm{b}}_{\mathrm{B}} \Delta D^{\mathrm{C}}_{\mathrm{c}} \Delta\sigma^{\mathrm{ab}\to\mathrm{cd}} \left[1 + \mathrm{O}(\alpha_{\mathrm{s}})\right] . \tag{58}$$

The symbol Δ denotes the difference in the corresponding quantities for different spin orientations in the initial and finite particles.

One-spin transverse asymmetries, at the constituent level in a hard subprocess, are nonzero in view of the vector nature of the interaction [44]. Thus, if the energy and the transverse momentum are sufficiently high that contributions from the higher twists may be neglected, one expects that $A_{\mathrm{N}} = 0$. Any departure from this prediction will necessitate a serious revision of perturbative QCD. Analogous to elastic scattering, discovery of nonzero transverse asymmetry in inclusive processes may be linked with the breaking of the chiral symmetry because spin properties are closely related to the chiral features of the theory.

The energy independence of Λ hyperons and their considerable polarisation in the 12 – 2000 GeV interval indicate that spin effects are important at very high energies as well [4]. Other experimental results, including large spin effects in elastic scattering at 28 GeV and large values of $p_{\perp}^2$ [3], provide further evidence in favour of this conclusion.

Since at Tevatron energies (for $\sqrt{s} = 2$ TeV) the higher-twist effects are negligible, it follows that measuring A_{N} might make it possible to test QCD, at large $p_{\perp}$ and for x_{F} close to zero, in processes such as

$$\mathrm{p}_{\uparrow} + \bar{\mathrm{p}} \to \pi + \mathrm{X} , \quad \mathrm{p}_{\uparrow} + \bar{\mathrm{p}} \to \mathrm{jet} + \mathrm{X} . \tag{59}$$

Such measurements of A_{N} would serve as a test of the very basis of QCD, i.e. of the Lagrangian of the standard model in the strong interaction region.

On the other hand, measurements of longitudinal asymmetries may give information about the production mechanism and spin structure of hadrons. One approach which seems to offer promise is the study of reactions with an unstable baryon in the final state, such as

$$\mathrm{p}_{\rightarrow} + \bar{\mathrm{p}} \to \Lambda_{\rightarrow} + \mathrm{X} . \tag{60}$$

For such a reaction, the subprocess $q\bar{q} \to s\bar{s}$ will dominate at large $x_\perp$, whereas the gluon annihilation, $gg \to s\bar{s}$, will provide a significant background at low values of $x_\perp$. It is thus seen for different kinematical regions that the process (60) is sensitive to the quark or gluon polarisation in a polarised proton.

Asymmetries at the constituent level are calculated within the perturbative QCD framework [46], so the measurements of, for example, the parameter D_{LL} yield information concerning quark and gluon polarisations. Theoretical estimates put D_{LL} at the 50% level [47]. The measurement of D_{LL} is also of interest from the viewpoint of strange-sea polarisation in the nucleon, which may be highly negative in accord with the EMC results.

4.2 Nonperturbative models for spin effects in inclusive processes

Turning back to the question of the ability or disability of QCD to describe spin effects, at not too high energies the situation is, admittedly, more complex. In fact in this region, in addition to large $p_\perp$ data, testing the theory also requires one to consider effects such as higher twists, hadron diquarks, interaction in the initial and final states, and chiral symmetry breakdown.

It has been argued [48] that the internal transverse momenta of the constituents must be included in the description of one-spin asymmetry. More precisely, the idea was to introduce structure functions dependent on partons' transverse momentum $\boldsymbol{k}_\perp$:

$$G_{\mathrm{H}}^{\mathrm{a}}(x, Q^2) \to G_{\mathrm{H}}^{\mathrm{a}}(x, \boldsymbol{k}_\perp, Q^2) \ . \tag{61}$$

The assumption of correlation between the proton spin and the orbital motion of proton constituents had earlier led to the prediction of a nontrivial asymmetry A_N in elastic scattering [49]. For large values of $p_\perp$ it is found that [49]:

$$A_{\mathrm{N}} \sim \frac{\langle k_\perp \rangle}{p_\perp} \ . \tag{62}$$

The important point here is that the expression for asymmetry does not involve either the mass quark or α_s. Nevertheless, this dependence of the asymmetry A_N on $p_\perp$ rules out the large values of one-spin asymmetry which are observed experimentally at large $p_\perp$.

In order to describe the one-spin asymmetry observed in a hadron production reaction on a polarised target, $A + B_\uparrow \to C + X$, the present authors [50] have developed a model which is based on the U matrix approach and also employs Chou–Yang's idea of rotating hadron matter (which is the quark condensate in this context). The asymmetry is related to the contribution from the condensate to the hadron spin which the latter, for a transverse hadron polarisation, may be represented as the sum

$$s_{\mathrm{h}} = s_{\mathrm{q}} + \langle L \rangle_{\mathrm{cond}} \ . \tag{63}$$

In the effective-field generation process, the orbital momentum of the condensate in the polarised hadron will be transferred to the cloud of the quarks produced by the interaction of the hadron condensates, i.e. the cloud will have its orbital momentum $\langle L \rangle_{\mathrm{cond}}$ different from zero, a feature which is naturally associated with the cloud's rotation. Thus, the origin of asymmetry in hadron production is related to the nonzero orbital momentum of the cloud of $q\bar{q}$ pairs.

The dependence of the asymmetry on energy and $p_\perp$ has the form

$$A_{\mathrm{N}}(s, p_\perp) = c \frac{\langle L \rangle_{\mathrm{cond}}}{s_{\mathrm{h}}} s^{-\alpha/2} \beta(p_\perp) \ , \tag{64}$$

$$\beta(p_\perp) = \begin{cases} p_\perp^{-n} \exp(p_\perp/m) \,, & p_\perp < p_\perp^0 \,, \\ \mathrm{const} \,, & p_\perp > p_\perp^0 \,, \end{cases} \tag{65}$$

where $m^{-1} \approx 1$ fm and $n = 8$ is the exponent with which the cross sections decays with $p_\perp$. The asymmetry A_N is proportional to the fraction of the total hadron spin which is associated with the orbital momentum of the condensate. The asymmetry is a decreasing function of the energy, the parameter α varying from 3 to 5.

Thus, not only perturbative QCD but also simple models involving nonperturbative QCD features predict low one-spin asymmetries in the hard region in high-energy inclusive processes. This observation, it is believed, will stimulate experiments on testing directly not only the predictions of particular theoretical models but also the very foundations of the modern theory of strong interactions.

5. Spin asymmetries in electroweak interactions

The title of this section covers an extremely broad subject area. We will only touch on some questions associated with the possibility of producing an accelerated, polarised proton beam. In this case the measurement of the longitudinal asymmetry A_L is of particular interest because we are dealing here with the production of $W^\pm$ and of heavy lepton pairs.

Direct calculations of W^+ and W^- production can be carried out within the Drell–Yan picture. The reactions which dominate at energies $\sqrt{s} \sim 1$ TeV are the quark–antiquark fusion processes, $u\bar{d} \to W^+$ and $\bar{u}d \to W^-$.

Within the framework of the standard model, W is a left current, and the asymmetry at the constituent level is a maximum. Therefore the asymmetry A_L is expressed in terms of the spin-average quark distribution $q(x, M_W^2)$ and the spin-dependent quark distribution $\Delta q(x, M_W^2)$. Thus, measuring A_L in the process

$$p_\rightarrow + \bar{p} \to W^\pm + X \tag{66}$$

gives an independent way (in addition to deep-inelastic scattering) to obtain the spin quark distribution Δq, because the spin-average distribution q is known from experiments on unpolarised particles.

Furthermore, if spin quark distributions are available from other experiments, the measurement of asymmetry in $W^\pm$ production may be used for testing the standard model. This also holds for the production of large-mass parton pairs. In such processes the expectation value of the asymmetry A_L reaches 60% – 80% in certain kinematic regions [47]. Note, however, that in measuring A_L in the hadron production of W in the Tevatron some complications arise because of the kinematic uncertainties involved [51].

The longitudinal asymmetry A_L is also sensitive to the new physics' departure from the standard model. For example, the minimal extension of the model which incorporates left–right symmetric interactions suggests the production of massive right-side $W_R^\pm$. The asymmetry $A_L(p_\rightarrow + \bar{p} \to W_R^\pm + X)$ will then be opposite in sign to the asymmetry $A_L(p_\rightarrow + \bar{p} \to W_L^\pm + X)$.

6. Compositeness

The measurement of A_L and A_N is also helpful in the search for compositeness. Today there exist many models which consider quarks and leptons as composed of further constituents (preons). The simplest indication of quark compositeness is that the jet production cross section at large transverse momenta departs from perturbative QCD predictions. This is known to be due to a new quark–quark interaction term induced by the quark composed structures,

$$L = \eta_0 \frac{g^2}{\Lambda_c^2} \bar{q} A q \bar{q} A q \ , \qquad (67)$$

where the compositeness scale Λ_c is of the order of the preon binding energy.

The form of A is determined by the particular model of the Dirac interaction structure. The parallel study of polarisation and the search for compositeness are important in that they make it possible to determine the type of the interaction, i.e. the form of A. Different forms of A, such as $A = \gamma^{\mu}(1 - \gamma^5)/2$ or $A = \gamma_{\mu}$, give almost identical predictions for cross sections averaged over the spin degrees of freedom [52]. However, predictions for the parameter A_L differ widely for the above versions of A.

7. Conclusion

Measurements of the spin structure function $g_1^p(x)$ have revealed the nontrivial spin structure of the proton. These results, together with the large spin effects observed in hard elastic and inelastic interactions, suggest further investigations in this area. UNK IHEP experiments with a polarised jet target and Tevatron FNAL experiments with a polarised proton beam will make it possible to study both the spin properties of interactions and the spin structure of the proton.

Collisions of polarised protons with antiprotons at $\sqrt{s} = 2$ TeV are going to offer new and unique possibilities. They will make it possible to test the basic present-day views on particle interactions and to continue the quest for a new physics beyond the framework of the standard model. Polarised beams are necessary in measuring the analysing power and spin–spin correlation at large $p_{\perp}^2$. Moreover, a polarised beam will be effective in reducing the background in studying rare processes such as top-quark production.

The study of spin effects, in particular the production of accelerated polarised beams, is a more complicated problem. Experience shows, however, that the measurement of spin-related observables always leads to new and unexpected results that provide further insight into the structure of particles and the dynamics of their interactions. The measure-ment of spin observables in high-energy hadron processes will, hopefully, justify the current theoretical views on the nature of strong interactions and will further our understanding of the quark interaction at large distances.

Acknowledgements. The authors are grateful to A A Logunov and Yu D Prokoshkin for their helpful interest in this work.

References

1. SLAC Yale Collaboration, *Phys. Rev. Lett.* **51** 1135 (1983); EMC Collaboration, *Nucl. Phys. B* **328** 1 (1989); *Phys. Lett. B* **206** 364 (1988); SMC Collaboration, *Phys. Lett. B* **302** 533 (1993); SLAC E142 Collaboration, SLAC Preprint, 1993
2. Brodsky S J, Invited lectures presented at the SLAC Summer Institute on Particle Physics: Spin Structure in High Energy Processes (Stanford, California, July 26–August 6, 1993)
3. Krisch A D, Plenary lecture given at the 9th Int. Symp. on High Energy Spin Physics (Bonn, Germany, September 1990)
4. Heller K, Invited talk given at the 7th Int. Symp. on High Energy Spin Physics (Protvino, September 1986)
5. Solovianov V L, Invited talk given at the 7th Int. Symp. on High Energy Spin Physics (Protvino, September 1986)
6. Adams D L et al. FERMILAB-Pub-91/14-E (Batavia, 1991)
7. Troshin S M, Tyurin N E *Spin v Fizike Vysokikh Energii* (Spin in High-Energy Physics) (Moscow: Nauka, 1991)
8. Mueller A (Ed.) *Pertubative Quantum Chromodynamics* (Singapore: World Scientific, 1987)
9. Bjorken J D, in *Proc. 3rd Int. Symp. on Electron and Photon Interactions, Stanford, California, 1967*; Feynman R P *Phys. Rev. Lett.* **23** 1415 (1969)
10. Troshin S M, Tyurin N E *Int. J. Mod. Phys. A* **5** 2689 (1990)
11. Brodsky S, Lepage P *Phys. Rev. D* **22** 2157 (1980)
12. Matveev V A, Muradyan R M, Tavkhelidze A N *Lett. Nuovo Cimento* **7** 719 (1973); Brodsky S, Farrar G *Phys. Rev. Lett.* **31** 1153 (1973)
13. Landshoff P V *Phys. Rev. D* **10** 1024 (1974)
14. Botts J, Sterman G *Nucl. Phys. B* **325** 62 (1989)
15. Pire B, Ralston J P *Phys. Lett. B* **117** 233 (1982)
16. Ramsey G P, Sivers D *Phys. Rev. D* **45** 79 (1992)
17. Manohar A, Georgi H *Nucl. Phys. B* **234** 139 (1984)
18. Brodsky S, de Teramond G *Phys. Rev. Lett.* **60** 1924 (1988)
19. Anselmino M, Kroll P, Pire B *Z. Phys. C* **36** 89 (1988)
20. Szwed J *Phys. Lett. B* **105** 403 (1981)
21. Goloskokov S V, in *Proc. 7th Int. Symp. on High Energy Spin Physics, Protvino, September 1986*
22. Kazaks P A, Tucker D L *Phys. Rev. D* **37** 222 (1988)
23. Preparata G, Soffer J *Phys. Lett. B* **86** 304 (1979)
24. Bourelly C, Soffer J *Phys. Rev. D* **35** 145 (1987)
25. Pondrom L, Invited talk given at the 7th Int. Symp. on High Energy Spin Physics (Protvino, September 1986)
26. Ellis J, Brodsky S J, Karliner M *Phys. Lett. B* **206** 309 (1988)
27. Troshin S M, Tyurin N E *Particle World* **3** 165 (1994)
28. Troshin S M, Tyurin N E *Part. Nucl.* **15** 53 (1984)
29. Ellwanger U, Stech B *Z. Phys. C* **49** 683 (1991); Fritzsch H *Phys. Lett. B* **235** 75 (1991)
30. Ball R D *Int. J. Mod. Phys. A* **5** 4391 (1990)
31. Islam M M *Europhys. Lett.* **4** 183 (1987); *Nucl. Phys. B* (Proc. Suppl.) **25** 104 (1992)
32. Nambu Y, Jona-Lasinio G *Phys. Rev.* **122** 345 (1961)
33. Meissner U G *Phys. Rep.* **161** 213 (1988)
34. Krisch A D *Phys. Rev. Lett.* **11** 217 (1963)
35. Orear J *Phys. Rev. D* **18** 2484 (1978)
36. Troshin S M, Tyurin N E, in *Proc. 6th Int. Seminar on High Energy Physics and Quantum Field Theory, Protvino, 1983* Vol. 2. p. 79; Troshin S M, Tyurin N E, Yuschenko O P *Nuovo Cimento A* **91** 23 (1986)
37. Klimt S, Lutz M, Vogl V, Weise W *Nucl. Phys. A* **516** 469 (1990); Povh B, Hufner J *Phys. Lett. B* **245** 653 (1990)
38. Troshin S M, Tyurin N E, in *Proc. Int. Workshop on Spin Phenomena at High Energies, Protvino, 1984* p. 167; Tyurin N E *Nucl. Phys. B* (Proc. Suppl.) **25** 91 (1992)
39. Logunov A A, Savrin V I, Tyurin N E, Khrustalev O A *Teor. Mat. Fiz.* **6** 157 (1971)
40. Dean N W *Nuovo Cimento A* **52** 1129 (1967); Martin A, Peshanski R *Phys. Rev. D* **18** 685 (1978); Schrempp B, Schrempp F, Preprint CERN TH-2573, 1978
41. Troshin S M, Tyurin N E *Sov. J. Part. Nucl.* **15** 25 (1984)
42. Troshin S M, Tyurin N E *Phys. Lett. B* **144** 260 (1984); *J. Phys.* (*Paris*) *Colloq.* 46, C2–235 (1985)

43. Hendry A W *Phys. Rev. D* **10** 2300 (1974)
44. Kane G L, Pumplin J, Repko W *Phys. Rev. Lett.* **41** 1689 (1978)
45. Collins J C, in *Proc. of the Conference on the Intersection of Nuclear and Particle Physics, Tucson, Arizona, May 1991*
46. Craigie N S, Hidaka K, Jacob M, Renard F M *Phys. Rep.* **99** 69 (1983)
47. Bourelly C, Soffer J, Renard F M, Taxil P *Phys. Rep.* **177** 319 (1989)
48. Sivers D *Phys. Rev. D* **41** 83 (1990)
49. Chou T T, Yang C N *Nucl. Phys. B* **107** 1 (1976)
50. Troshin S M, Tyurin N E *Z. Phys. C* **45** (1989); Preprint IHEP 91-163 (Protvino, 1991)
51. Pondrom L, Private communication
52. Hinchliffe I *Proc. 1984 Summer Study on the Design and Utilization of the Superconducting Super Collider, Snowmass, 1984* p. 1